Fe$_{65.5}$Cr$_4$Mo$_4$Ga$_4$P$_{12}$C$_5$B$_{5.5}$ BMGs: Sample preparation, thermal stability and mechanical properties

M. Stoica [a,b,*], J. Eckert [c], S. Roth [a], A.R. Yavari [b], L. Schultz [a]

[a] *IFW Dresden, Institute for Metallic Materials, P.O. Box 270016, D-01171 Dresden, Germany*
[b] *LTPCM-CNRS UA29, ENSEEG, Institut National Politechnique de Grenoble, Domain Universitaire,
1130 Rue de la Piscine, BP 75 Saint Martin d'Hères Campus, 38402 Grenoble, France*
[c] *TU Darmstadt, Department of Materials and Geo Sciences, Physical Metallurgy Division,
Petersenstraße 23, D-64287 Darmstadt, Germany*

Available online 6 October 2006

Abstract

Bulk amorphous Fe-based alloys with the nominal composition Fe$_{65.5}$Cr$_4$Mo$_4$Ga$_4$P$_{12}$C$_5$B$_{5.5}$ have been obtained by copper mold casting in different shapes: cylindrical rods with diameters up to 3 mm, rectangular bars of 2 mm × 2 mm and discs of 10 mm diameter and 1 mm thickness. These alloys exhibit good soft magnetic properties, characterized by low coercivity and high saturation magnetization. Besides the magnetic properties, the Fe$_{65.5}$Cr$_4$Mo$_4$Ga$_4$P$_{12}$C$_5$B$_{5.5}$ bulk metallic glass (BMG) shows a high glass transition temperature T_g, as well as a high crystallization temperature T_x, with an extension of the supercooled liquid region of around 65 K. The mechanical behavior was investigated by compression and Vickers hardness tests. The fracture strength for the as-cast samples σ_f is 2.8 GPa and the fracture strain ε_f is 1.9%. Upon annealing at 715 K for 10 min, i.e. at a temperature below the calorimetric glass transition, the fracture strain drops to 1.6% and no plastic deformation is observed. The Vickers hardness H_V for the as-cast samples is about 885, and increases to 902 upon annealing. The fracture behavior of these Fe-based bulk glassy alloys is significantly different in comparison with the well-studied Zr-, Cu- or Ti-based good glass-formers. The fracture is not propagating along a well-defined direction and the fractured surface looks irregular. Instead of veins, the glassy alloy develops a high number of microcracks.
© 2006 Elsevier B.V. All rights reserved.

Keywords: Amorphous materials; Thermal analysis

1. Introduction

Because of the absence of crystalline anisotropy, Fe$_{65.5}$Cr$_4$Mo$_4$Ga$_4$P$_{12}$C$_5$B$_{5.5}$ amorphous alloys exhibit good soft magnetic properties, characterized by a low coercive force and a high permeability. Nevertheless, residual anisotropies may be present, such as shape anisotropy or stress-induced anisotropies, caused by internal mechanical stresses induced during the preparation procedure [1,2]. Using the copper mold casting method, such alloys can be cast in form of bulk specimens directly suitable for use as magnetic sensors, magnetic valves or magnetic clutches. But for possible use in magnetic devices, the Fe-based BMGs also require good mechanical strength besides the good soft magnetic properties.

The critical cooling rate of about 100 K/s necessary for glass formation of magnetic BMGs is higher than the value of about 1–10 K/s characteristic for non-magnetic alloys with very good glass-forming ability [3,4]. Thus, the maximum achievable diameter of these Fe-based alloys is limited to only a few millimeters [5], in contrast to Zr- or Cu-based glassy alloys, which can easily reach 10 mm diameter [6]. Only very recently, Ponnambalam et al. [7] and, independently, Lu et al. [8] succeeded to cast Fe-based BMGs with a thickness larger than one centimeter (using some small additions of Y, Ln and/or Er), but their glasses are paramagnetic at room temperature, with a Curie temperature of around 55 K. The difficulty to cast such ferrous glasses in bulk form is one of the reasons for which, despite an increasing number of published papers on the mechanical properties of BMGs, most of these reports deal only with non-ferrous Zr-, Ti- or Cu- based alloys [6,9,10]. The mechanical properties of bulk Fe-based glasses started to be investigated only in the past few years [7,8,11–13]. The known strength values for non-ferrous glassy alloys are in the range of: 1.5–1.8 GPa for Zr-based alloys, 1.7–1.9 GPa for Ti-based alloys, 1.9–2.5 GPa for Cu-based

---

* Corresponding author. Present address: Leibniz Institute for Solid State and Materials Research (IFW) Dresden, PO Box 270016, D-01171 Dresden, Germany. Tel.: +49 351 4659 644; fax: +49 351 4659 452.

E-mail addresses: m.stoica@ifw-dresden.de, mstoicaro@yahoo.com (M. Stoica).

alloys or 2.7–3.1 GPa for Ni-based alloys (for an overview, see [12]). For our $Fe_{65.5}Cr_4Mo_4Ga_4P_{12}C_5B_{5.5}$ BMG, the fracture strength exceeds 2.8 GPa. In the case of Zr- or Cu- based bulk glassy alloys, the fracture usually proceeds along a shear plane, which is declined by ∼45° to the direction of the applied load, and the fracture surface exhibits a well-developed vein pattern [6,10]. In contrast, the studied $Fe_{65.5}Cr_4Mo_4Ga_4P_{12}C_5B_{5.5}$ samples develop a cleavage-like fracture surface with a high number of microcracks, which finally destroy the sample completely. The fracture surface appears to contain a high number of small fracture zones, which are probably generated at the same time due to the very high stress level upon deformation.

2. Experimental

The preparation of the amorphous $Fe_{65.5}Cr_4Mo_4Ga_4P_{12}C_5B_{5.5}$ BMGs was done in several steps. First, master alloy ingots were obtained by induction melting using Fe–B, Fe–C, Fe–Ga, Fe–P pre-alloys and pure elements as Mo (99.4% purity), Cr (99.95% purity), Fe (99.9% purity) and crystalline B (99.99% purity). Induction melting of Fe with B, Fe with C (99.9% purity) and Fe with Ga (99.7% purity) allowed to produce the respective pre-alloys. The FeP pre-alloy was obtained by induction melting of consolidated powder resulted upon milling Fe powder (99.9% purity, less than 10 μm particle size) with amorphous red P powder (99% purity, less than 100 μm particle size)

Amorphous rods with diameters of 1.5, 2, 2.5 and 3 mm, length of 70 mm, rectangular bars of 2 mm × 2 mm with length of 30 mm as well as discs of 10 mm diameter and 1 mm thickness were prepared from the master alloy with nominal composition $Fe_{65.5}Cr_4Mo_4Ga_4P_{12}C_5B_{5.5}$. The samples were obtained by induction melting under argon atmosphere at a pressure of 80 KPa and subsequent injection into a copper mold under an applied pressure of 3×10^5 Pa. Because the presence of oxides can have a negative influence in order to prepare bulk amorphous alloys, we checked the oxygen content of the pre-alloys and of the master alloy. This revealed very low values: 180 ppm for Fe-P, 130 ppm for the other pre-alloys and 50 ppm for $Fe_{65.5}Cr_4Mo_4Ga_4P_{12}C_5B_{5.5}$, respectively.

The thermal stability, i.e. the glass transition, the extension of the supercooled liquid region and the crystallization, was examined by differential scanning calorimetry (DSC), using a Netzsch DSC 404 under argon flow. The glass transition temperature T_g and the crystallization temperature T_x were measured as the onset temperatures of the glass transition and the crystallization events, respectively, during heating with a constant rate of 40 K/s. The extension of the supercooled liquid region, defined as the difference between the glass transition temperature and the crystallization temperature, $\Delta T_x = T_x - T_g$ was also calculated. Additionally, the melting temperature T_m defined by the liquidus temperature T_{liq} at the onset of melting upon heating with the same constant rate of 40 K/s was measured. The amorphous structure as well as the crystallization behavior and the magnetic properties of these glassy samples have already been investigated and published previously [14–17].

In order to investigate the mechanical behavior, different techniques were used. First, room temperature compression tests using an electromechanical Instron 8562 testing device were performed for as-cast rods of 2 and 2.5 mm diameter, respectively, as well as for as-cast and annealed 2 mm × 2 mm rectangular bars. The length of the samples was between 4 and 5 mm and the machine was operated in the constant position rate mode, with a displacement of 10^{-3} mm/s. The corresponding strain rate was evaluated as 10^{-4} s^{-1}. From the compression tests, the fracture strength σ_f, the fracture strain ε_f, the yield strength σ_y, the yield strain ε_y and the Young's modulus E were derived.

The Vickers hardness was measured for the same kind of bar samples using a computer controlled Struers Duramin 5 hardness tester. The tests were performed using a typical diamond indenter in the form of pyramid with square base and an angle of 136° between opposite faces, applying a load of 1.96 N for 10 s. The diagonal of the imprints as well as the hardness were calculated using a Digital Video Measuring System. For indentations, the samples were embedded in epoxy resin and the measured surface was carefully polished with a paste containing diamond particles with a diameter smaller than 0.25 μm. The characteristics of the fractured surface as well as the features of the indents after the hardness tests

Table 1
Glass transition temperatures T_g, crystallization temperatures T_x and liquidus temperatures T_{liq}, as well as reduced glass transition temperatures $T_{rg} = T_g/T_{liq}$, γ parameter, extension of the supercooled liquid region ΔT_x and crystallization enthalpy ΔH_x for as-cast $Fe_{66.5}Cr_4Mo_4Ga_4P_{12}C_5B_{5.5}$ glassy alloys measured at 40 K/min heating rate

Sample	Rod (Ø 1.5 mm)	Rod (Ø 2 mm)	Rod (Ø 2.5 mm)	Rod (Ø 3 mm)
T_g (K)	746	749	750	751
T_x (K)	812	814	814	815
T_{liq} (K)	1344	1347	1346	1346
T_g/T_{liq}	0.55	0.55	0.55	0.55
γ	0.388	0.388	0.388	0.388
ΔT_x (K)	66	65	64	64
ΔH_x (J/g)	69.6	67.8	65.1	56.1

were studied by scanning electron microscopy (SEM), using a JEOL JSM 6400 microscope operated at 25 kV.

3. Results and discussion

The glass-forming ability (GFA) can be evaluated from thermal stability measurements. Usually, high values of the extension of the supercooled liquid region ΔT_x and the reduced glass transition temperatures $T_{rg} = T_g/T_{liq}$ indicate a good GFA [9]. The values for T_g, T_x and T_{liq} as a function of geometrical dimensions of the as-cast rods are given in Table 1. Using these values, ΔT_x and T_{rg} were calculated. Recently, Lu and Liu [18,19] proposed a new parameter γ defined as $T_x/(T_g + T_{liq})$, to predict GFA for various glass-forming systems. Usually, the γ values of BMGs range between 0.35 and 0.50 [18].

The glass transition temperature and the crystallization temperature slowly increase with increasing rod diameter. The differences in thermal stability between rods with different diameters are caused by a different degree of relaxation as a result of the different cooling rates reached during solidification. Another reason can be a slightly variation in actual composition of the glasses. Such compositional variations may arise if at least the rods with larger diameters are not fully amorphous but contain some (nano)crystalline phase(s), which may form (i)- due to a possible appearance of crystalline nuclei in the liquid state, or (ii)- due to an insufficient cooling rate for complete glass formation upon casting. Some crystalline inclusions can form from the molten state and, upon casting, the already formed crystalline clusters may or may not act as seeds for further nucleation. Thus, the composition of the remaining matrix is slightly different from the starting overall composition and this can modify the thermal stability data. Concerning the second hypothesis, the cooling rate decreases with increasing diameter of the cast rods and thus the maximum achievable diameter for which the sample is still amorphous is limited. Hence, the rod most susceptible to contain some crystalline inclusions should be the rod with the largest diameter. The presence of crystalline inclusions was observed in the case of 3 mm diameter rod; in a previous work [14] we have described in detail the formation of such crystalline clusters by means of time-resolved X-ray diffraction in transmission configuration using a high-energy high intensity monochromatic synchrotron beam.
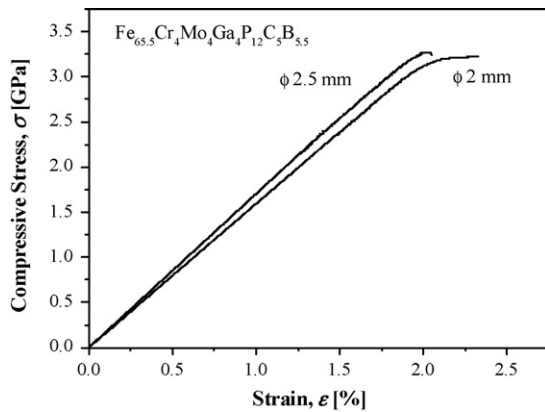
Fig. 1. Compressive stress–strain curves for as-cast $Fe_{65.5}Cr_4Mo_4Ga_4P_{12}C_5B_{5.5}$ 2 and 2.5 mm diameter rods.

Fig. 2. Compressive stress–strain curves for $Fe_{65.5}Cr_4Mo_4Ga_4P_{12}C_5B_{5.5}$ as-cast and annealed 2 mm × 2 mm rectangular bars.

A small decrease of the crystallization enthalpy ΔH_x with increasing rod diameter can be observed. This can also be an indication that the rods with larger diameters are susceptible to contain some frozen-in crystalline nuclei. However, the differences between the values are relatively small and within the measurements errors.

The extension of supercooled liquid region of around 65 K and the reduced glass transition temperature of around 0.55 is characteristic for good glass forming systems. It is, however, in the lower limit when compared with the ratio 0.57–0.72 measured in the $(Pd,Ni,Cu)_{80}P_{20}$ and $(Pd,Ni,Fe)_{80}P_{20}$ glass systems, which are two of the best glass forming systems known [4,20,21].

Lu and Liu [18] linked the new dimensionless γ parameter to the critical cooling rate R_c as well as to a critical cross section Z_c by studying the data available in literature for representative non-ferrous BMGs. Using γ parameter equal to 0.388 (Table 1), the calculated critical cooling rate is 91 K/s and the maximum achievable diameter 2.9 mm. According to the data reviewed by Inoue [6], the Fe-based BMGs of the composition Fe–Cr–Mo–Ga–P–C–B should achieve a thickness of a few mm and the critical cooling rate is of the order of hundreds K/s. The calculated values are somehow lower, but the errors are acceptable.

Fig. 1 shows the compressive stress–strain curves for the as-cast $Fe_{65.5}Cr_4Mo_4Ga_4P_{12}C_5B_{5.5}$ cylindrical rods with 2 and 2.5 mm diameter, respectively. Both samples exhibit similar features, i.e. an elastic deformation regime followed by a small compressive plastic strain. The yield stress σ_y, measured at the offset yield, is 3.19 GPa in the case of the 2 mm diameter sample and 3.27 GPa for the 2.5 mm diameter sample. The corresponding elastic strain ε_y is 2.03% for the 2 mm diameter rod and 1.91% for the 2.5 mm diameter rod, respectively. Young's modulus is determined as 160 GPa for the 2 mm diameter sample and 170 GPa for the 2.5 mm diameter sample. The fracture of the samples occurs at a fracture stress σ_f of 3.23 GPa for the 2 mm diameter sample. σ_f reaches 3.27 GPa for the 2.5 mm diameter sample. The fracture strain ε_f is 2.33 and 2.03%, respectively. The pure compressive plastic strain is 0.30 and 0.12% for the two samples, respectively. Hence, this Fe-based bulk glass exhibits
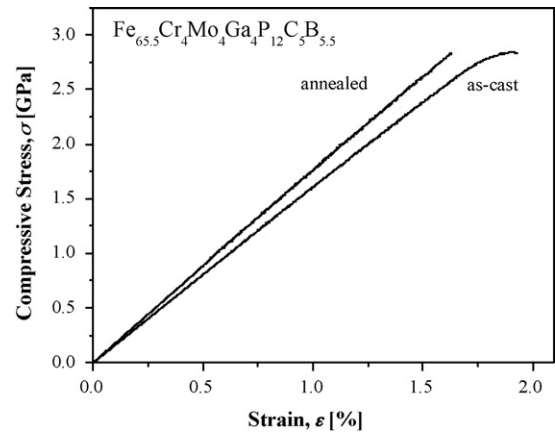
a very high strength, higher than that observed in the case of non-ferrous bulk amorphous alloys [12], but close to that measured for Fe–B–Si–Nb (3.25 GPa) and Fe–Ga–P–C–B–Si systems (3.16 GPa) [11].

The differences between the two described samples regarding their mechanical data are quite small and are within the limits of error of the measurement. The error in the measurement of the small cross-section of the sample is 5% and is comparable with the difference between the two calculated values for Young's modulus (160 GPa for the 2 mm and 170 GPa for the 2.5 mm diameter sample, respectively).

Fig. 2 shows the compressive stress–strain curves for as-cast and annealed rectangular bars with the cross section 2 mm × 2 mm. The samples were annealed for 10 min at 712 K, i.e., at a temperature equal to T_g—15 K, using a heating and cooling rate of 5 K/min (for rectangular bars, $T_g = 727$ K, measured in DSC at 5 K/min heating rate). It can be noted that the fracture stress retains almost the same value after annealing, but the sample becomes more brittle and no plastic deformation is observed. The yield stress is 2.82 and 2.84 GPa for the as-cast and for the annealed sample, respectively. The corresponding compressive elastic strains are 1.76 and 1.60%, respectively. Young's modulus is 161 GPa for the as-cast state and 177 GPa after annealing. The fracture of both samples occurs at nearly the same value of compressive stress, 2.84 GPa, but the corresponding fracture strain is different: 1.91% for the as-cast sample and 1.63% for the annealed one. The as-cast sample shows a small plastic deformation of 0.15%, but in the case of the annealed bar the plastic regime extends only over 0.03%.

The appearance of the fracture surface was investigated by SEM. Fig. 3(a and b) show micrographs of the $Fe_{65.5}Cr_4Mo_4Ga_4P_{12}C_5B_{5.5}$ as-cast rectangular bar after fracture at different magnifications. The observed fracture behavior is totally different from that observed for Zr- or Cu- based bulk glassy alloys, where the fracture usually proceeds along the maximum shear stress plane, which is declined by about 45° to the direction of the applied load, and the fracture surface contains a number of a well-developed vein patterns [6,10]. Fig. 3(a) shows a side view of the fractured sample. There are no distinct veins and dimples, at least not over the whole fracture surface but
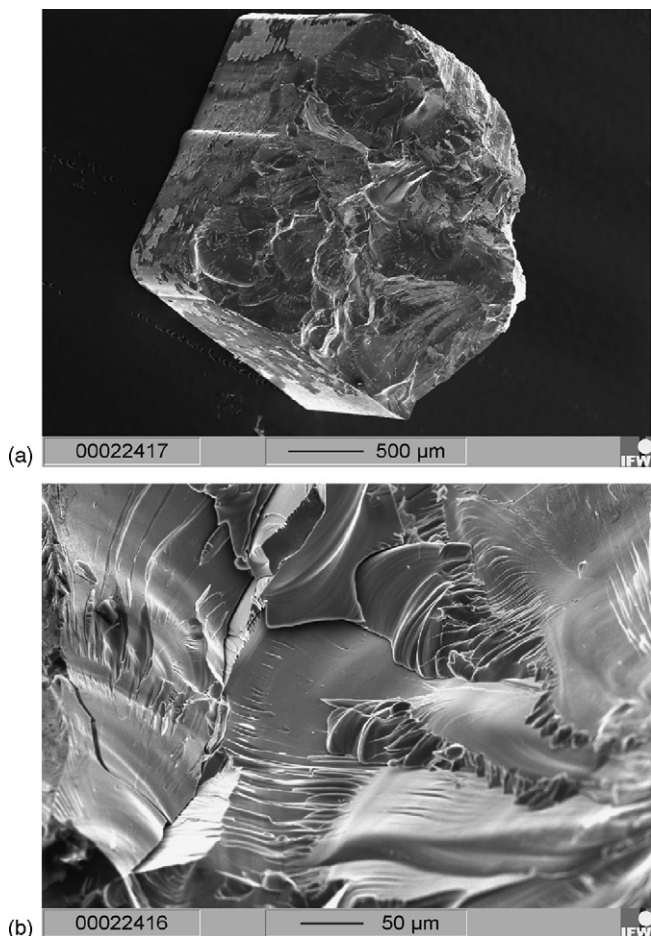
Fig. 3. SEM micrograph (topological view) showing the fracture surface after compression test: (a) side view and (b) detail at higher magnification.

only in some regions. Recent systematic investigations on the glasses with different alloy systems indicate that the shear fracture always deviates from the maximum shear stress plane either under compression or under tension [22]. For the samples studied here, the fracture surface appears to consist of a high number of small fracture zones, which leads to breaking of the samples into many small parts, as indicated in Fig. 3(b). It indicates that the fracture of metallic glasses can occur either in a shear mode or in a break mode, depending on the constituent elements and microstructure in detail. The actual failure mode of a metallic glassy sample is a competition result between shear fracture and distensile fracture as reported by Zhang et al. [23]. For the Fe-based glasses, it has quite high fracture strength, indicating that the critical shear fracture stress must be high enough in comparison to the bonding force among the constituent elements in the present glass. The brittleness can be also enhanced by the presence of metalloids, i.e. C, B and P [2]. Inoue et al. [11] supposed that such cracks as presented in Fig. 3(b) are relatively easy to be initiated nearly simultaneously because the stress level is very high, around 3 GPa, and the shock wave caused by initiation of one crack induces the generation of other cracks at different sites. The high strength of the Fe-based bulk glassy alloys seems to originate from the high bonding forces between the constituent elements. This is in agreement with the relatively

high value found for T_g, because is considered that T_g reflects the bonding nature between the constituent elements [24].

The Vickers hardness was measured for the same kind of as-cast and annealed rectangular bar samples with the cross section 2 mm × 2 mm as used for compression tests. For the as-cast bars, H_V is 885 (8.68 GPa) with a typical standard deviation of 5. The hardness of the annealed bars increases up to $H_V = 902$ (8.84 GPa) with a standard deviation of 2.1. The smaller value of the standard deviation in the case of the annealed samples indicates a more homogeneous behavior of the annealed specimens in comparison with the as-cast state. Upon indentation, some slips generated by the Vickers diamond indenter and the absence of any visible crack can be noticed (picture not presented here). These features are in accordance with the elastic-plastic behavior found from the compression test.

The ratio σ_f/E attains values of around 0.017 and $H_V/3E$ takes values of 0.018 and 0.016 for the as-cast and annealed samples, respectively. Hence, the relationship between the fracture strength and the hardness $\sigma_f \approx H_V/3$ is verified [2]. Considering that a number of amorphous alloys reported up to date have nearly fixed values of about 0.02 for σ_f/E and $H_V/3E$ [2], it is concluded that the studied Fe-based bulk glassy alloys follow the same trend. The agreement also suggests that the Fe-based bulk glassy alloys have an elastic-plastic deformation mode similar to other non-ferrous bulk glassy alloys, the main difference being a much higher strength level, which can be achieved in compression tests.

4. Conclusions

The bulk amorphous $Fe_{65.5}Cr_4Mo_4Ga_4P_{12}C_5B_{5.5}$ samples with various shapes produced by copper mold casting exhibits a good GFA and a high thermal stability. A high strength and some compressive plastic strain was observed upon compression test performed at room temperature. A structural relaxation treatment at elevated temperature does not affect the stress level, which remains almost the same, but the plasticity disappears. The fracture mechanism is different in our Fe-based bulk glassy alloy in comparison with other non-magnetic metallic glasses. The actual failure mode of metallic glassy sample is a competition result between shear fracture and distensile fracture.

Acknowledgements

References

[1] A. Inoue, J.S. Gook, Mater. Trans. JIM 36 (1995) 1180.
[2] H.S. Chen, Rep. Prog. Phys. 43 (1980) 353.

[3] A. Inoue, A. Kato, T. Zhang, S.G. Kim, T. Masumoto, Mater. Trans. JIM 32 (1991) 609.

[4] Y. He, T. Shen, R.B. Schwarz, Metall. Mater. Trans. A 29 (1998) 1795.

[5] A. Inoue, T. Zhang, A. Takeuchi, Appl. Phys. Lett. 71 (1997) 464.

[6] A. Inoue, Acta Mater. 48 (2000) 279.

[7] V. Ponnambalam, S.J. Poon, G.J. Shiflet, J. Mater. Res. 19 (2004) 1320.

[8] Z.P. Lu, C.T. Liu, J.R. Thomson, W.D. Porter, Phys. Rev. Lett. 92 (2004) 245503.

[9] A. Inoue, Bulk Amorphous Alloys, Trans Tech Publications, Uetikon-Zuerich Switzerland, 1999.

[10] A. Inoue, W. Zhang, T. Zhang, K. Kurosaka. Acta Mater. 49 (2001) 2645.

[11] A. Inoue, B.L. Shen, A.R. Yavari, A.L. Greer, J. Mater. Res. 18 (2003) 1487.

[12] A. Inoue, B.L. Shen, H. Koshiba, H. Kato, A.R. Yavari, Acta Mater. 52 (2004) 1631.

[13] A. Inoue, X.M. Wang, Acta Mater. 48 (2000) 1383.

[14] M. Stoica, J. Eckert, S. Roth, L. Schultz, A.R. Yavari, Å. Kvick, J. Metastable Nanocryst. Mater. 12 (2002) 77.

[15] M. Stoica, J. Degmová, S. Roth, J. Eckert, H. Grahl, L. Schultz, A.R. Yavari, Å. Kvick, G. Heunen, Mater. Trans. 43 (2002) 1966.

[16] M. Stoica, J. Eckert, S. Roth, L. Schultz, Mater. Sci. Eng. A 375–377 (2004) 399.

[17] M. Stoica, S. Roth, J. Eckert, L. Schultz, M.D. Baró, J. Magn. Magn. Mater. 290–291 (2005) 1480.

[18] Z.P. Lu, C.T. Liu, Acta Mater. 50 (2002) 3501.

[19] Z.P. Lu, C.T. Liu, Phys. Rev. Lett. 91 (2003) 115505.

[20] R.B. Schwarz, Y. He, Mater. Sci. Forum 235–238 (1997) 231.

[21] T.D. Shen, Y. He, R.B. Schwarz, J. Mater. Res. 14 (1999) 2107.

[22] Z.F. Zhang, J. Eckert, L. Schultz, Acta Mater. 51 (2003) 1167.

[23] Z.F. Zhang, G. He, J. Eckert, L. Schultz, Phys. Rev. Lett. 91 (2003) 045505.

[24] F.R. De Boer, R. Boom, W.C.M. Mattens, A.R. Miedema, A.K. Niessen, Cohesions in Metals, North-Holland, Amsterdam, The Netherlands, 1989.